Investigation of the s-shape caused by the hole selective layer in bulk heterojunction solar cells - Supplemental material

Lothar Sims[a,b,*], Ulrich Hörmann[a], Robert Hanfland[a], Roderick C.I. MacKenzie[c], F. René Kogler[d], Roland Steim[e], Wolfgang Brütting[a], Pavel Schilinsky[b]

[a]*University of Augsburg, Institute of Physics, Universitätsstr. 1, 86135 Augsburg, Germany*

[b]*Belectric OPV GmbH, Landgrabenstr. 94, 90443 Nürnberg, Germany*

[c]*Faculty of Engineering, University of Nottingham, Nottingham, NG7 2RD UK*

[d]*Konarka Technologies GmbH, Landgrabenstr. 94, 90443 Nürnberg, Germany*

[e]*Laboratory for Functional Polymers, Empa Swiss Federal Laboratories for Materials Science and Technology, Überlandstr. 129, 8600 Dübendorf, Switzerland*

S 1 Mobility and charge transport in the HSL

S 1.1 Mobility measurements

S 1.1.1 Transfer characteristic of OFETs

presents the transistor drain current (I_d), plotted as a function of gate voltage (V_g) with fixed drain voltage. For pure, pristine TPD layers no drain current is visible even at high negative

* Corresponding author.
E-mail address: lothar.sims@physik.uni-augsburg.de (L.Sims)

gate voltages since the drain current is below our measurement sensitivity. Note that some devices show ambipolar behavior, which indicates that electrons are present in the transistor above certain gate voltages. In particular, the pure HATCN FET solely shows n-type behavior. A repeated measurement of the pure TPD film after storage for 500 hrs in nitrogen atmosphere clearly shows a drain current using the same range for the gate voltage and same value for the drain voltage as before.

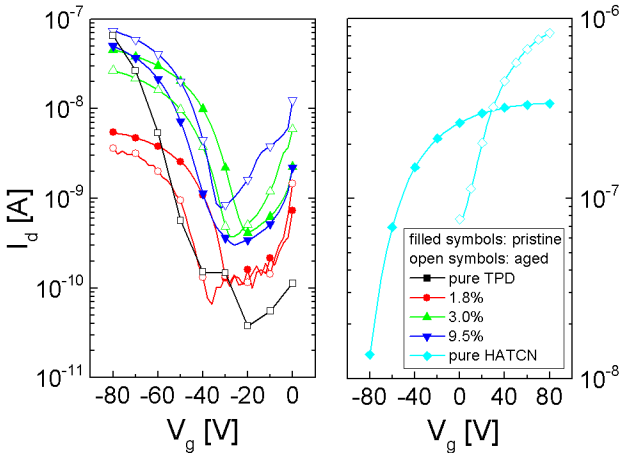

Figure S 1 - Transfer characteristics of all samples in a nitrogen atmosphere before (filled symbols) and after storage of 500 hrs (open symbols). For the pristine pure TPD sample no drain current could be measured since it was below the measurement limit of around $2x10^{-7}cm^2/Vs$.

.

S 1.1.2 Mobility of pristine TPD

In literature, a broad range of mobilities for pure TPD is found, strongly depending on the measurement technique [S1],[S2],[S3]. Assuming our mobility of the lowest HATCN concentration as a lower measurement limit and considering the general trend of increasing mobility with increasing HATCN content, we roughly estimate the mobility of the pristine TPD film to be around $1x10^{-7}$ cm^2/Vs.

S 1.2 Charge transport mechanisms in TPD:HATCN

S 1.2.1 Multiple-trapping-and-release model

On the one hand there is the multiple-trapping-and-release model [S4]. A possible consequence of co-evaporation of HATCN with TPD might be that low lying states in the tail of the Gaussian distribution are filled up with charges and are thus no more available for other charges. The probability for charges moving through TPD of being trapped is reduced which in turn leads to an increased mobility [S5].

S 1.2.2 Distance of HATCN molecules

On the other hand HATCN could serve as additional transport channel once the concentration is high enough. To estimate the distance from HATCN-to-HATCN molecule an equal distribution of TPD and HATCN molecules with a radius of 0.5nm [S6] for both over the volume of the HSL layer is assumed. The total number of molecules N_{total} within the layer with volume V and molecule volume V_m is

$$N_{total} = \frac{V}{V_m} \qquad \text{(S 1)}$$

The number of HATCN molecules N_H depends on the ratio n of HATCN in the layer

$$N_H = N_{total}\, n \qquad \text{(S 2)}$$

The volume around each HATCN molecule V_a where no other HATCN molecule can be found is

$$V_a = \frac{V}{N_H} \qquad \text{(S 3)}$$

Since the V and N_H are directly proportional the radius r_a of V_a depends solely on the molecule's radius r_m and the ratio n

$$r_a = \frac{r_m}{n^{1/3}} \qquad \text{(S 4)}$$

The distance of two HATCN molecules is $2r_a$. The number of HATCN molecules inside the HSL and their distance is given in Table S 1

Table S 1 - Distance of HATCN molecules

Sample	N_H	Distance [nm]
1.8 % HATCN	4.81×10^{12}	3.8
3.0 % HATCN	8.02×10^{12}	3.2
9.5 % HATCN	2.54×10^{13}	2.2

The largest transfer integral is obtained for 1 nm center-to-center distance (i.e. the molecules are touching). Due to the exponential decreasing transfer energy the probability for direct hopping of charges from HATCN to HATCN molecule is rather small [S7].

S 1.3 Simulation

The device model was fit to the light JV curve of the device with the pure HATCN contact layer, by taking values for the material parameters which were already published in the literature for the P3HT:PCBM material system and then allowing the model to vary these parameters until a good fit was found [S8]. The device was assumed symmetric to reduce the number of free parameters. After allowing the device parameters to vary the following fit parameters were found to reproduce the light JV-curve:

Free carrier to trapped carrier cross section $2.50 \times 10^{-20} m^{-3}$. Recombination cross section $5 \times 10^{-24} m^{-2}$. Exponential tail states were assumed with an energetic distribution of 60×10^{-3} meV, the density of these trap states at the band edge were assumed to be $2 \times 10^{26} m^{-3} eV^{-1}$, the effective density of free states was taken as $5 \times 10^{26} m^{-3}$, and the charge on the contacts was taken as $2 \times 10^{26} m^{-3}$.

When the mobility of the HSL was lowered an s-shaped JV curve was produced. It is important to note that we do not state that these are the exact material parameters of the real device. We only say that they are a set of parameters which can reproduce the light JV curve of the device with the pure HATCN layer. The important point is that we obtain the generic result, that an s-shaped JV curves is produced when the mobility of the HSL is reduced.

References

[S1] A. Kuwahara, S. Naka, H. Okada, H. Onnagawa, Carrier mobility of organic thin films using lateral electrode structure with optical slits, Appl. Phys. Lett. 89 (2006) 132106. doi:10.1063/1.2352731.

[S2] M. Aonuma, T. Oyamada, H. Sasabe, T. Miki, C. Adachi, Material design of hole transport materials capable of thick-film formation in organic light emitting diodes, Appl. Phys. Lett. 90 (2007) 183503. doi:10.1063/1.2733627.

[S3] K. Kudo, Nanotechnology and Nano-Interface Controlled Electronic Devices, Elsevier Science B.V., Amsterdam, 2003.

[S4] R. Schmechel, Hopping transport in doped organic semiconductors: A theoretical approach and its application to p-doped zinc-phthalocyanine, J. Appl. Phys. 93 (2003) 4653–4660.

[S5] S. Olthof, S. Mehraeen, S.K. Mohapatra, S. Barlow, V. Coropceanu, J.-L. Brédas, et al., Ultralow Doping in Organic Semiconductors: Evidence of Trap Filling, Phys. Rev. Lett. 109 (2012) 176601. doi:10.1103/PhysRevLett.109.176601.

[S6] D.M. Goodall, E. Bergström, M. Surve, Separation, size and charge determination of small molecules using CE in combination with UV area imaging, Chromatogr. Today. (2010) 31–34.

[S7] R.C.I. MacKenzie, J.M. Frost, J. Nelson, A numerical study of mobility in thin films of fullerene derivatives, J. Chem. Phys. 132 (2010) 064904. doi:10.1063/1.3315872.

[S8] R.C.I. MacKenzie, C.G. Shuttle, M.L. Chabinyc, J. Nelson, Extracting Microscopic Device Parameters from Transient Photocurrent Measurements of P3HT:PCBM Solar Cells, Adv. Energy Mater. 2 (2012) 662–669. doi:10.1002/aenm.201100709.